

**CCD photometry of neglected southern hemisphere short period contact
Eclipsing Binary stars RV Gru, BC Gru and RW PsA**

ABSTRACT

This project was part of a collaborative pro-am program to study neglected southern contact eclipsing binaries of type EW (W Ursae Majoris), initiated by the Variable Stars South (VSS). Three stars, RV Gru, BC Gru and RW PsA, were observed over a period of 2 to 5 weeks to determine their light elements. All three targets were successfully measured and the results were consistent with published values. Differences between observed and published periods were RV Gru: 0.000063, BC Gru: -0.00006, RW PsA: 0.000019 days. Primary minimum magnitude for RV Gru needs further study as it was observed at 0.35 V lower than published value which is 10 times the measurement uncertainty.

1. Introduction

Astronomers study binary star systems because they provide a convenient tool for the exploration of some of the fundamental properties of their component stars such as mass, diameter and temperature. In addition their orbital parameters, period, semi-major axis orbital inclination are also determinable.

Eclipsing binary stars are a class of binary stars with orbital plane in approximate alignment with our line of sight and we see them vary in brightness as they periodically pass in front of each other. They are mostly in close orbits and we study their variations in brightness using photometry. Because observing and recording lightcurves using modern CCD based photometry requires only modest equipment, amateur astronomers contribute the bulk of observation to variable star research as members of major collaborative professional-amateur (pro-am) organisations such as AAVSO (American Association of Variable Star Observers) and VSS (Variable Stars South).

The genesis of this project was a request for serious amateurs to join a pro-am project at VSS to observe long neglected Type EW (W UMa) southern eclipsing binaries. (VSS-EW-web).

Type EW (also called W Ursae Majoris) variable stars are a member of a group of eclipsing binaries which include EA (Algol type), EB (semi-detached binaries) and EW (contact binaries) and their subgroups. (AAVSOweb)

Fig 1. shows the three types of eclipsing binaries and their typical lightcurves:

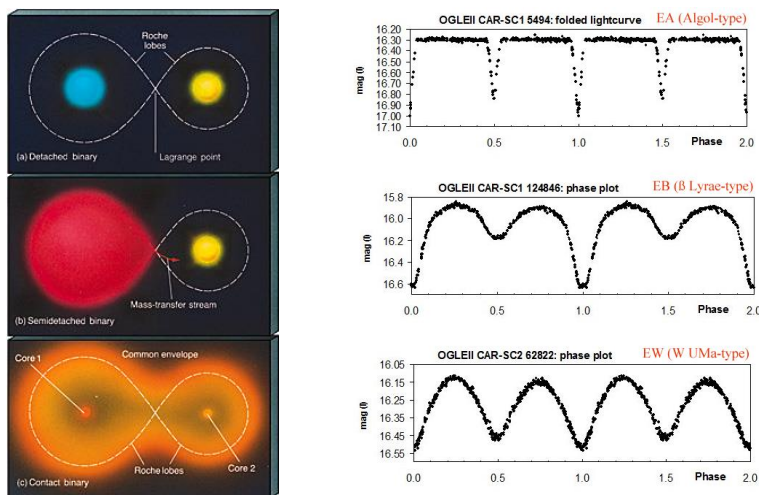


Fig 1a & 1b. Eclipsing binary star schematics and sample associated lightcurves
 Credit : 1a. Nanjing University 1b.VSOB (Variable Star Observers Bulletin)

Binary stars in close orbits, have either one or both of their shapes gravitationally deformed into ellipsoids or teardrops. Their individual rotation rates are gradually synchronised by frictional braking as they rotate through the gravitationally induced bulge dissipating rotational and orbital energy. The process continues until the system reaches minimum energy and circular orbit while conserving its angular momentum. (Ostlie 2007). The two stars then rotate and orbit together as a rigid body.

In Fig 1a. the figure-eight dotted outline depicts the cross section of the gravitational equipotential surface surrounding the Roche lobes of the two stars. Eclipsing binaries are defined by how the two Roche lobes are filled by the stars. If the separation is much greater than either of the radii, the stars are largely spherical and behave as normal main sequence stars then this system is called detached, Algol or EA type eclipsing binary. As the stars evolve, one of the stars, normally called the secondary, expands and eventually fills its Roche lobe and starts spilling material into the Roche lobe of the primary through the shared equipotential Lagrangian point L_1 where the two Roche lobes touch. This system is called semi-detached or EB type. Either the primary or the secondary can be the more massive star. If the primary star also expands to fill its Roche lobe the two stars share a common atmosphere bounded by a dumbbell-shaped equipotential surface, the system is called a contact binary. These are the EW type binaries. The stars can expand past this point and overspill their Roche lobes and become over-contact eclipsing binaries. (The use of ~~over-contact~~ as a separate class has been discontinued on advice from the IAU (Wilson 2001))

Table 1. summarises some of the main properties of eclipsing binaries.

Type (prototype)	Period(days)	Spectral type	^a M_V (amplitude)
EA (Algol)	0.2 - >10000	any	0 . several Mag
EB (Lyrae)	> 0.5	B - A	< 2 (V)
EW (W UMa)	< 1	F - G	< 0.8 (V)

Table 1a. Main properties of eclipsing binary star types. Adopted from AAVSO VSX

Currently there are several accepted subtypes of contact binaries. With specific characteristics listed in table 1b.

Subtype	Period (days)	Spectral type	Identifying Characteristics	Reference
EW A	0.4 . 0.8	A - F	T1 > T2	Binnendijk 1965
EW W	0.22 . 0.4	G or K	T1 < T2	Binnendijk 1965
EW B			T1 >> T2	Lucy&Wilson 1979
EW H			q > 0.72	Csizmadia 2004

Table 1b. Main properties of EW (W UMa) eclipsing binary star types. q is mass ratio.

The objectives of this project involves the photometric observation and the analysis of the lightcurves of type EW (W Ursa Majoris) eclipsing binaries only.

2. Observing Eclipsing Binaries

The astronomer's ultimate aim in observing eclipsing binaries is to determine their basic properties such as their masses m_1 and m_2 the mass of the primary and secondary respectively, their radii r_1 and r_2 , their surface temperature T_1 and T_2 , their separation d and the inclination of their orbit to the line of sight. Their individual luminosities L_1 and L_2 and therefore the distance can also be determined. This wish list is only achievable if both the photometric properties (bolometric lightcurve) and spectrographic Doppler shift (velocities) are observable. When spectroscopic observations are possible the system could be a single line or double line spectroscopic binary depending on whether the line spectrum of both components are observable or not. The Doppler shift of the line spectra enables the calculation of radial velocities v_{1r} and v_{2r} . If both spectra are observable the ratio and sum of the masses of the components are given by (from Keplers 3rd law)

$$m_1/m_2 = v_{2r}/v_{1r}$$

$$m_1+m_2 = (P/2\pi G)(v_{1r}+v_{2r})^3 / \sin^3 i$$

where P is orbital period, i is inclination of the orbit (90° for along line of sight) and individual masses can be calculated.

If only one spectrum is observable then neither the ratio nor the sum of the masses is solvable but the following expression for the *mass function* has been found to be useful (Ostlie 2007):

$$m_2^3 \sin^3 i / (m_1+m_2)^2 = (P/2\pi G) v_{2r}^3$$

Unfortunately for most cases especially for close binaries such as contact binaries, the subject of this project, line spectra is not available and photometry yielding a lightcurve in multiple spectral bands, such as UBVRI, is the only useful observable.

Because of their geometry, contact eclipsing binaries of the EW type have a lightcurve where it is not possible to identify the onset and end of transits and eclipses (Lucy 1968) which would enable the calculation or relative diameters.

Fig. 2 shows the theoretical light curve of an eclipsing contact binary star.

From the lightcurve it is possible to determine the bolometric magnitudes, maximum $m_{\text{bol},0}$, primary minimum $m_{\text{bol},p}$, and secondary minimum $m_{\text{bol},s}$. From these magnitudes, the ratio of the flux of the two components can be calculated and thence, using Stefan-Boltzmann's law, the ratio of surface temperatures is given by $T_s/T_l = (F_{rs}/F_{rl})^{1/4}$ where T_s and T_l are the surface temperatures of the smaller and the larger stars respectively and F_{rs} and F_{rl} . Apart from the orbital period, no other parameters of the system can be deduced directly from the lightcurve.

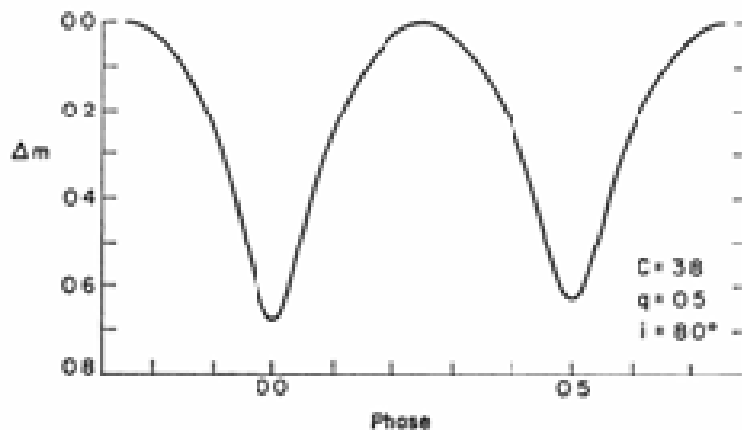


Fig 2. Theoretical light curve generated from proposed shape of rotating contact eclipsing binary of type EW (U Ma). Adopted from Lucy (1968)

To solve the lightcurve for the system's parameters m_1 , m_2 , (or $q_{\text{ph}} = m_1/m_2$), R_1 , R_2 , d and i , astronomers use computer models that simulate the system based on the assumed mathematical shape, the dumbbell. The lightcurve is solved by incrementally adjusting the parameters until the simulated lightcurve matches the observed.

There are a host of codes i.e. software, available for modeling eclipsing binary stars available to researchers in the field of eclipsing binary stars. They are mostly based on the original algorithm and code by Wilson & Devinney. (1971) Some examples lightcurve modeling software are:

Phoebe (Physics of Eclipsing Binaries) <http://phoebe-project.org/>
 Starlight Pro (SLP) (Screenshot shown in Fig 3.)
 Binary Maker 3.0 by Contact Software

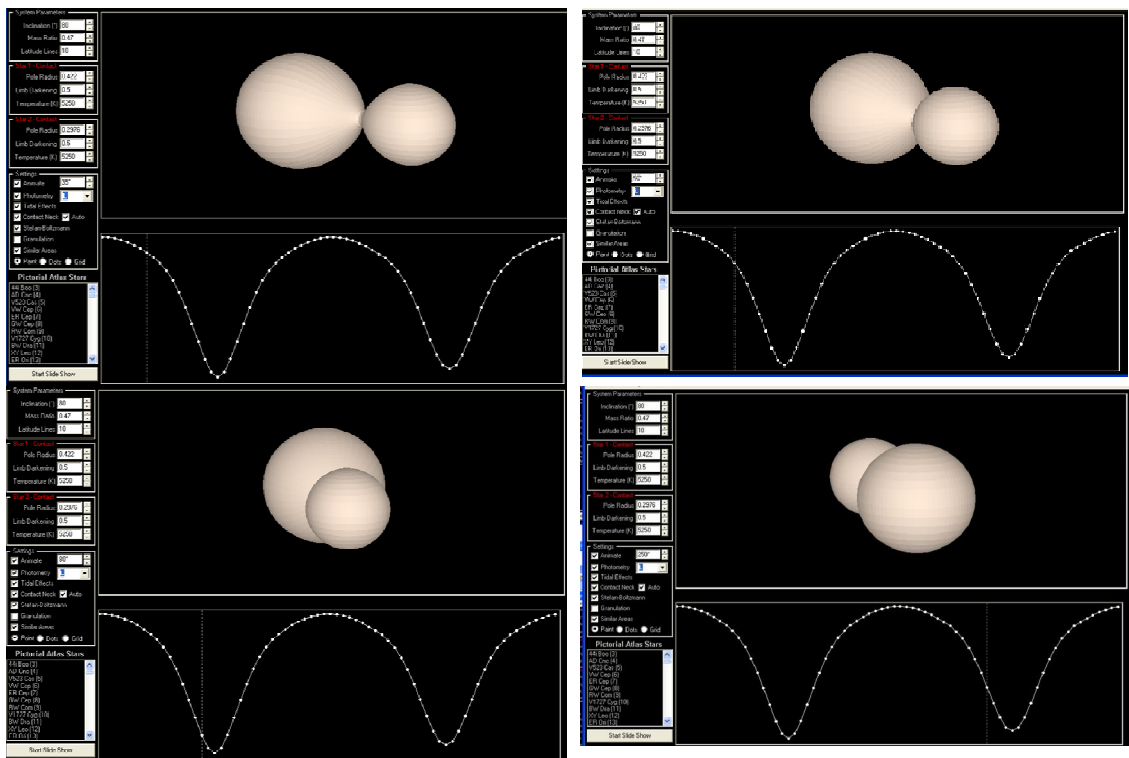


Fig 3 Screen shot of Starlight Pro. The parameters entered are used to generate the animation and the lightcurve.

As stated above, the objectives of this project are concerning only the photometric observation of contact binary (type EW - W Ursae Majoris) to obtain lightcurves of certain targets, analyse the lightcurve to extract light element, P (period), ToM (epoch-the time of minimum) and the amplitude of magnitude variations. V_{max} , V_{min_p} and V_{min_s}).

3. Target Selection

The selection of targets for this project were determined primarily by a list of poorly observed EW systems published in the VSS (Variable Stars South) newsletter 2015-3 (Richards 2015a).

Star	HJD0-2400000	Period	SpType	RA2000	DE2000	V_{max}	V_{min}
V743 Sgr	48393.82	0.276636	G8/K0V	17 43 56	-28 28 42	13.19	13.83
FS CrA	44826.55	0.263638	K3	18 06 12	-37 30 54	13.8	14.6
AB Tel	45885.46	0.325965		18 37 36	-50 57 48	13.4	14.1
BF Pav	49219.62	0.302319	G8V	18 45 36	-59 38 42	11	11.9
V902 Sgr	49191.95	0.293946	G9V	19 25 16	-29 08 54	14.4	14.8
LT Pav	45991.67	0.393672	F8V	19 48 36	-71 01 30	11.4	12.2
HY Pav	47023.81	0.351656	K1V	20 23 47	-73 42 12	11.42	12.16
ST Ind	44843.72	0.401916	F5V	20 35 24	-48 19 20	11.3	11.79
RW PsA	46675.7	0.360451	G6V	22 09 47	-27 04 02	11.05	11.76
RV Gru	46674.92	0.259516		22 39 24	-46 52 32	11	11.4
BC Gru	48479.93	0.307357	G8V	22 44 45	-48 09 50	10.6	10.94

Table 2. Targets proposed by Tom Richards of VSS Credit Pribulla 2003

EW binaries listed were such that the time of optimum observability roughly coincided with the semester timeframe of this project. That is about 9 weeks between first week of September and second week of November. From this list the targets were selected on the basis of the following criteria:

- Cordinates- centered on RA 22hr DEC. -20 °
- Period < 0.4 days
- Amplitude >0.3 V

The period needed to be as short as possible so that a significant part of a full cycle could be observed on a single night with the maximum chance of obtaining a primary minimum (ToM). For neglected short period eclipsing variables the available ephemerides could not be trusted as some of them have not been observed for decades, some since their discovery. The amplitude (Vmax-Vmin) was also an important consideration. While the available equipment was known to be capable of a magnitude scatter of less than 0.02V on a very good night, the average it is no better than ~0.05V. To be able to measure a light curve on an average night the amplitude needed to be >0.3.

From the original list shown in Table 2. the following three were finally chosen as targets for this project.

Star	2000	2000	Period	Vmax	Vmin
BC Gru	22 4 45	-48 09 50	0.3073	10.6	10.94
RW PsA	22 09 47	-27 04 02	0.3604	11.05	11.76
RV Gru	22 39 24	-46 52 32	0.2595	11	11.4

Table 3. Final target selection

4. Equipment

Arcadia is a small private amateur observatory dedicated to hunting for asteroids and normally used for confirmation astrometry of newly listed Near Earth Objects (NEOs) on the Minor Planet Centre (MPC) NEOCP web page. The equipment listed below was used in this project

Celestron model C14 Schmidt-Cassegrain Telescope (SCT), 14+(350mm) f/11 optics. Lumicon Giant Easy-Guider is used as a focal reducer for wide angle (FOV 25x19) imaging at F/7 and f=2520mm. Original fork mount is now equipped with custom made computer controlled drive electronics. The telescope can be operated remotely with semi GOTO capability over a private LAN (Local Area Network) from the on-site residence.

The auto-guider system for long exposure photography uses a piggy-back 150mm Newtonian guide scope and an SBIG SG4 standalone auto-guide camera. The system is capable of guiding on magnitude 11 stars with an accuracy of ~ 1+

The CCD camera is an SBIG ST8300M TEC cooled to about 30 degrees below ambient temperature. The Kodak KAF8300 CCD chip has 6 megapixels of size $5.4 \times 5.4 \mu\text{m}$, with 2x2 and 3x3 pixel binning available



Fig 3a. Arcadia Observatory equipment



Fig 3b Arcadia Observatory (Credit A. Hidas)

Software used for the project:

- Peranso 2.40 Light curve analysis software from Tonny Vanmunster
- MPO Canopus photometry software from Brian Warner
- Astrometrica astrometry/photometry software from Herbert Raab
- CCDOps camera control software from SBIG
- Guide 7 planetarium software from Project Pluto

5. Experimental Technique

Filter-less aperture photometry was used to measure the apparent visual magnitudes of the target stars in the CCD images as the aim was only to obtain accurate light elements for each target. Filters for this project were not required. (Richards 2015b).

Photometry from CCD images involves measuring counts of photoelectrons in the pixels representing the light flux of the object point source and converting them to an apparent magnitude by calibration using available comparison or reference stars in the image. *Absolute photometry* producing standardised multiband magnitudes requires careful pre-processing of raw CCD images to remove pixel non-uniformities with bias frames and rectifying optical system faults with flat field frames. Photometry of variable stars and asteroids for recording lightcurves where only the shape and magnitude

differentials are involved, *differential photometry*, or simple aperture photometry using catalogue based reference stars is sufficient.

Astrometrica by Herbert Raab is well known and widely used for astrometry. While *Astrometrica* reports magnitudes for astrometry to a precision of only 0.01 it has a comprehensive photometry function reporting magnitudes to a precision of 0.001 using reference stars from a nominated catalogue. The selected catalogue is accessed on line and image is calibrated automatically. Due to extensive experience with this software *Astrometrica* was used for photometry instead of MPO Canopus even though it may have been more appropriate for this purpose. While MPO Canopus was available and used to double check the lightcurve analysis that was done mostly on Peranso, it was not used for photometry due to the steep learning curve involved and the pressure of the semester timeframe. *Astrometrica's* catalogue based photometry computes true magnitudes without the need for hand picked comparison stars required by MPO Canopus. The quotation from Herbert Raab below describes the process in *Astrometrica*.

'Astrometrica performs aperture photometry on all reference stars (and on the target object). Using the magnitudes from the reference star catalog, Astrometrica performs a least square fit to find the zero point that fits all reference stars best. (Reference with magnitudes very different from the catalog magnitude are rejected from the fit.) Once the zero point has been determined, the software can calculate the magnitude of the target from the measured flux.' (Raab 2015)

The USNO UCAC 4 catalogue was selected for this project.

- Equipment setup

A focal reducer was used to match the image scale to the dimensions and configuration of the CCD chip. The Kodak CCD chip has a layout of 3326 x 2504 5.4x5.4 μ m pixels. For the given optical configuration and for increased sensitivity 3x3 binning is used for astrometry. The typical seeing at Arcadia results in star images of about 4+FWHM (Full Width Half Maximum). At the reduced 2520mm focal length of the telescope, the 3x3 binned pixels (measuring 16.2x16.2microns) project 1.32+ on the sky therefore using about 3 pixels to span a star image. This is considered ideal match by Herbert Raab (*AstrometricaWeb*).

Exposure was set by trial and error such that the maximum SNR was achieved without saturation. Pixel saturation was visible as a flat top on the plot of flux on *Astrometrica's* Object Verification screen (Fig 4.). As all targets were about the same magnitude (11V) 6-8 seconds was found to suitable exposure.

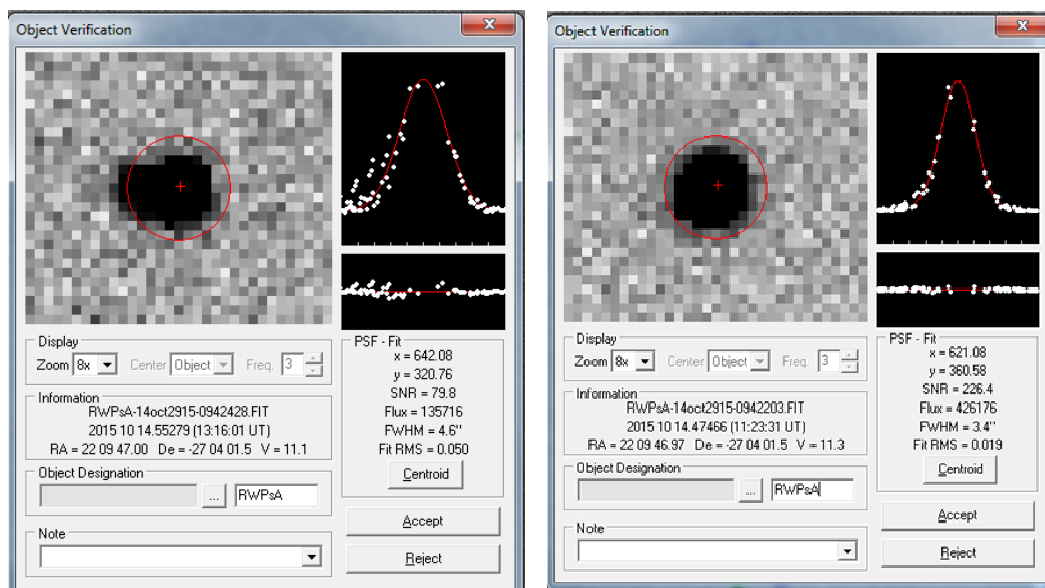


Fig. 4 Image PSF Gaussian fit in Astrometrica showing the effect good and bad image

- Observing Routine

As with all observational astronomy the weather controls the timing of any observation session. The expectation of at least 3 hours of clear skies was the usual trigger for an observing session. The usual observing routine was:

- Wait for forecast of clear weather that will last all night.
- Move telescope to the co-ordinates of the target. Check on *Guide 7* (planetarium software) to confirm that the target is in the field. Adjust the telescope focus using the focus function of CCDops camera control software. Activate auto-guiding.
- Take 20 images for quality control. CCDops does the initial image processing including automatic dark frame acquisition and subtraction on the fly. Load into photometry software *Astrometrica* to check star image quality using the Image Verification function that shows (Fig 4.) the quality of Gaussian fit to the image PSF (Point Spread Function), SNR, FWHM and the RMS (Root Mean Square) error of the fit. Readjust the focus if necessary. Start the long run. 300 to 600 images were taken at each session. Periodic check was made of image quality during the session and focus occasionally adjusted. Tracking was not an issue as auto-guiding was used even for the short exposures involved.
- Most of the initial image reduction was done during observing sessions, uploading large batches periodically to another computer over the LAN inside the onsite residence. The processing in *Astrometrica* was done 20 images at a time generating 20 lines of text data in the format shown in Fig. 5

OBSERVER: A. Hidas
 CONTACT: Andras Hidas [ash255@tpg.com.au]
 TELESCOPE: 0.35-m f/7.0 Schmidt-Cassegrain + CCD
 EXPOSURE JD: Mid-exposure, not corrected for light time

```

-----
      JD          mag          SNR          ZeroPt          Design.
-----
2457310.90269    11.583 V    499.15    25.482    RWPsA
2457310.90303    11.536 V    428.25    25.419    RWPsA
2457310.90338    11.568 V    424.22    25.450    RWPsA
2457310.90373    11.585 V    452.69    25.447    RWPsA
2457310.90407    11.532 V    443.99    25.403    RWPsA
2457310.90442    11.558 V    462.65    25.431    RWPsA
2457310.90477    11.412 V    443.57    25.376    RWPsA
    
```

Fig 5. Astrometrica photometry output format

The photometry data was loaded 20 measurements at a time into an Excel spreadsheet and inspected for magnitude scatter using the standard deviation () as a measure of quality. A for the batch of 20 of 0.05 was acceptable, 0.02 was good. Any group of 20 with > 0.07 was examined for an outlier (a value more than 3 from the mean) and removed.

Table 4 shows the summary of data collected.

Target	Nights observed	Span of days observed	No of images used
RV Gru	4	32.18	1481
BC Gru	5	19.07	1823
RW PsA	3	13.14	1478

Table 4. Observation summary

6. Data Reduction and Analysis

The primary objective of the project was the acquisition the *light elements* of the target stars from the lightcurve. The basic light elements are the period of revolution or orbital period of the eclipsing binary and an epoch or a reference time, normally considered as any time of minimum brightness (ToM) in the lightcurve. Also of interest is the amplitude of brightness change and the actual apparent brightness. As the orbital period may vary over the medium and long term, astronomers also keep track of these changes on the O-C plot. The O-C plot charts the difference between the observed minimum (O) and the calculated minimum (C). The calculated minimum is derived from ephemerides which use the simple expression (MtSohuraWeb)

$$HJD = HJD_0 + P E \text{ (Kreiner 2000).}$$

Where *HJD* is Heliocentric Julian Day of predicted minimum, *HJD₀* is epoch of a past minimum (or last observation) and *P* is period in days at that epoch. *E* is an integer used for calculating future minima. The ephemerides used in this project for RV Gru

and RW PsA were from MtSohuraWeb: <http://www.as.up.krakow.pl/o-c/>. Ephemerides for BC Gru were calculated manually using the expression above and light elements from AAVSO VSX.

The raw data, following inspection and the removal of obvious outliers in the Excel spreadsheet, consists of a number of text files, one for each night of observation, each file representing a segment of the target lightcurve. Each line of text, point on the lightcurve, represents JD (Julian Day), apparent magnitude V , and magnitude error estimate. The magnitude error estimate is derived from the SNR using the expression $e=V/SNR$. SNR comes from the *Astrometrica* output. Only one dataset (for RV Gru) spanned a full lightcurve cycle in one night. Other datasets spanned variable proportions of a full lightcurve over multiple nights with most nights including a ToM (Time of Minimum) so a satisfactory phase coverage was achieved for all targets.

On suggestion from VSS (Richards 2015b) Peranso 2.40 was used for lightcurve analysis. It has proven to be extremely easy, user friendly, while producing consistent, reproducible results.

ToMs from each lightcurve segment were extracted using the `extrema` search feature in Peranso and the JD converted to HJD using applet on the BAA (British Astronomical Association) website (BritastroWeb). Heliocentric JD (HJD) refers timing of events as if measured from the centre of the solar system to compensate for light time to Earth from different parts of its orbit. Without this correction, `epoch` could be in error by up to 0.00579 days or 8.3 minutes.

Minima and maxima magnitudes were estimated by taking the mean of ten observations on either side of the extrema found by Peranso. The error was estimated by calculating $1/\sqrt{20}$ ($\sim 1/4.5$) of the 20 data points around extrema.

The period of lightcurves were computed by Peranso from the total phase coverage of all observations of the target. There are several algorithms available in Peranso to choose from, the choice depending on what type of lightcurves, variable star types and asteroids are being analysed. For this project the Fourier based Lomb-Scargle method was used. This method best suits unevenly spaced data which characterises these observations. (Vanmunster 2004).

7. Detailed Results

The following pages present a summary of data analysis for each target:

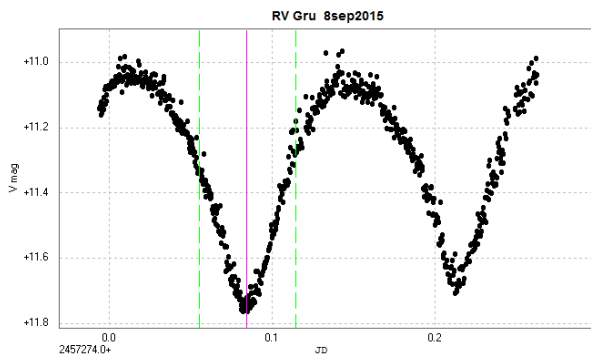
For each nights a lightcurve and the table of parameters measured (ToM, V_{min} , V_{max} and error estimates) are shown. For each ToM the ephemeris (predicted time) and the difference (O-C) are also presented.

The last two diagrams for each target present the results of Lomb-Scargle period analysis; the *phase plot* showing all data folded over a single period and the frequency plot with the dominant frequency marked and labeled: F (frequency) and P (period).

The period (P) in days is calculated from the frequency displayed and is given by:

$P = 2/F$ where F is shown on the graph. The factor 2 is required because the frequency analyzer assumes (correctly) that the 1st half of the lightcurve should be of identical duration to the 2nd half. The estimated uncertainty associated with the dominant frequency was taken from the related information screen and converted to the error in the full period.

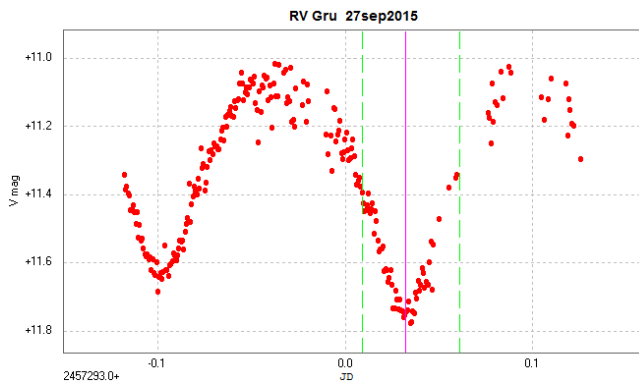
- RV Gru**



RV Gru

ToM (pri) HJD	Ephemeris HJD ₀	O-C (d)	Vmin (pri)	Vmax
2457274.08904	2457274.07977	0.00927	11.74	11.05
+/- 0.0001			+/- 0.005	+/-0.01

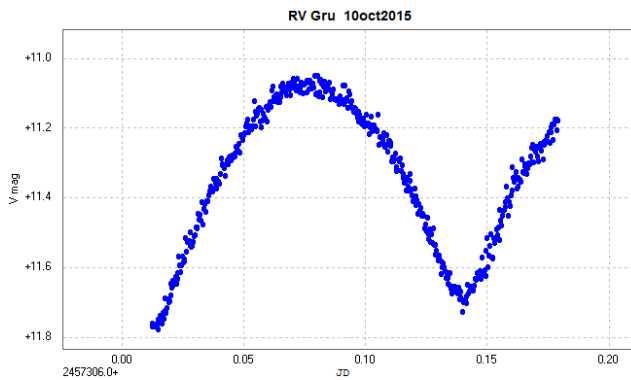
Fig. 6 Lightcurve plot and measures of RV Gru 08 Sep 2015



RV Gru

ToM (pri) HJD	Ephemeris HJD ₀	O-C (d)	Vmin (pri)	Vmax
2457293.03618	2457293.02445	0.01173	11.75	11.08
+/- 0.0001			+/-0.01	+/-0.02

Fig. 7 Lightcurve plot and measures of RV Gru 27 Sep 2015



RV Gru

ToM (pri) HJD	Ephemeris HJD ₀	O-C (d)	Vmin (pri)	Vmax
2457306.01663	2457306.00026	0.01637	11.76	11.07
+/- 0.0001			+/- 0.012	+/-0.02

Fig. 8 Lightcurve plot and measures of RV Gru 10 Oct 2015

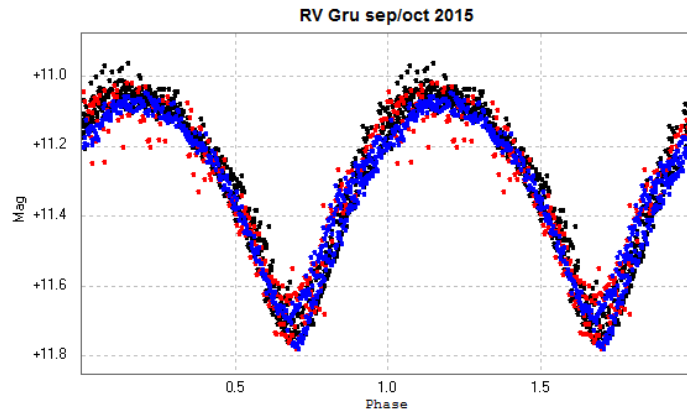


Fig 9 Phase plot of RV Gru

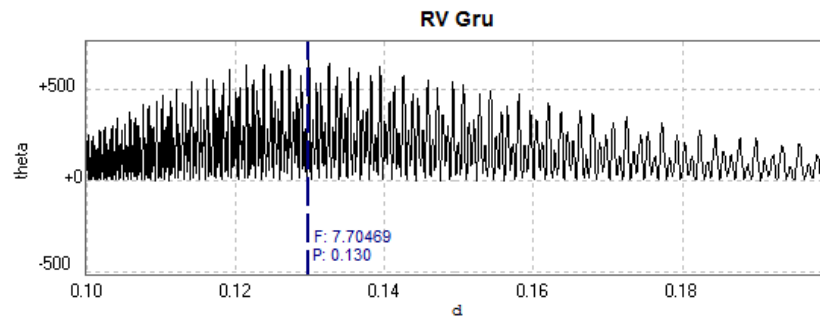
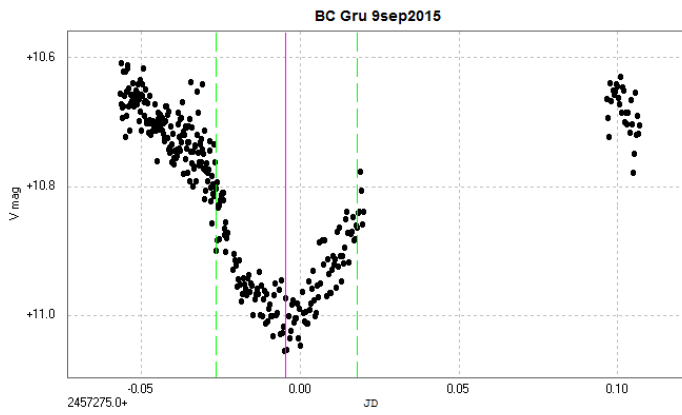


Fig 10. Frequency plot of RV Gru showing dominant frequency

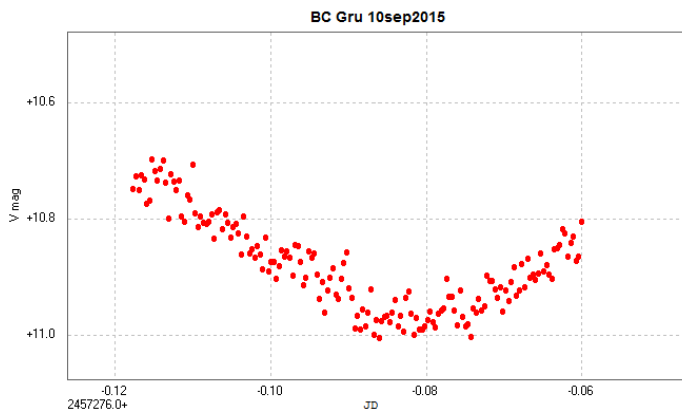
- BC Gru**



BC Gru

ToM (pri) HJD	Ephemeris HJD ₀	O-C (d)	Vmin (pri)	Vmax
2457274.99981	2457274.94315	0.05556	11.00	
+/-0.0001			+/-0.01	

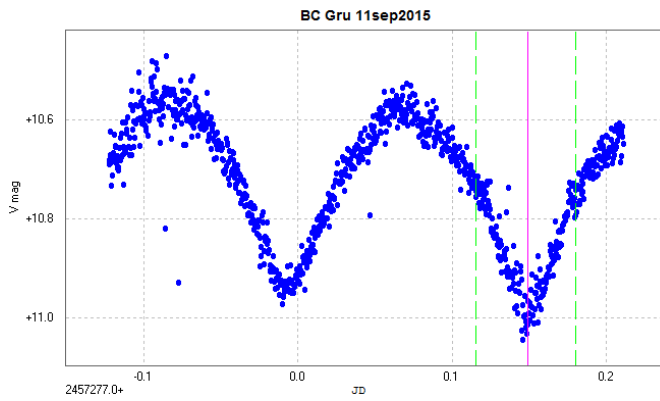
Fig. 11 Lightcurve plot and measures of BC Gru 9 Sep 2015



BC Gru

ToM (pri) HJD	Ephemeris HJD ₀	O-C (d)	Vmin (pri)	Vmax
2457275.92126	2457275.86522	0.05604	10.97	
+/-0.0002			+/-0.01	

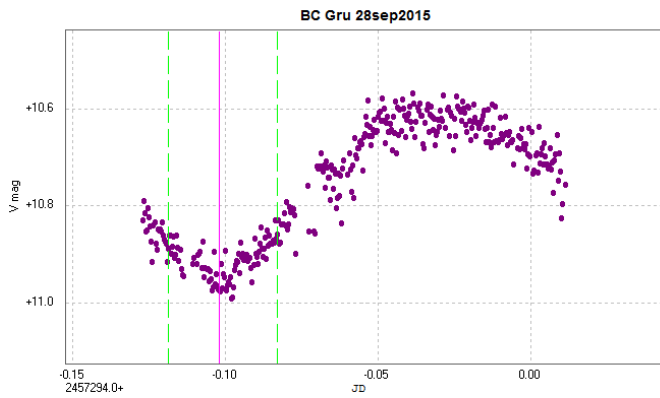
Fig. 12 Lightcurve plot and measures of BC Gru 10 Sep 2015



BC Gru

ToM (pri) HJD	Ephemeris HJD ₀	O-C (d)	Vmin (pri)	Vmax
2457277.15343	2457277.09465	0.05878	11.00	10.58
+/-0.0018			+/-0.01	+/-0.01

Fig. 13 Lightcurve plot and measures of BC Gru 11 Sep 2015



BC Gru

ToM (pri) HJD	Ephemeris HJD ₀	O-C (d)	Vmin (pri)	Vmax
2457293.90138	2457293.84559	0.05579		10.62
+/-0.002				0.01

Fig. 14 Lightcurve plot and measures of BC Gru 28 Sep 2015

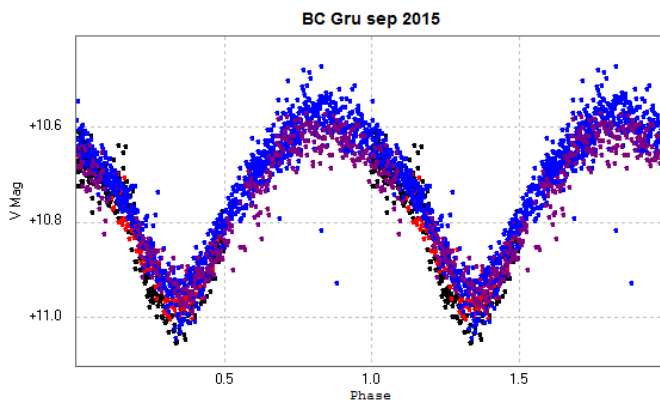


Fig 15 Phase plot of BC Gru

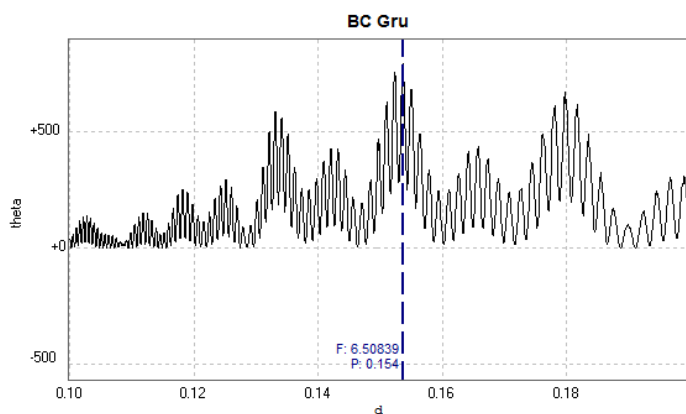
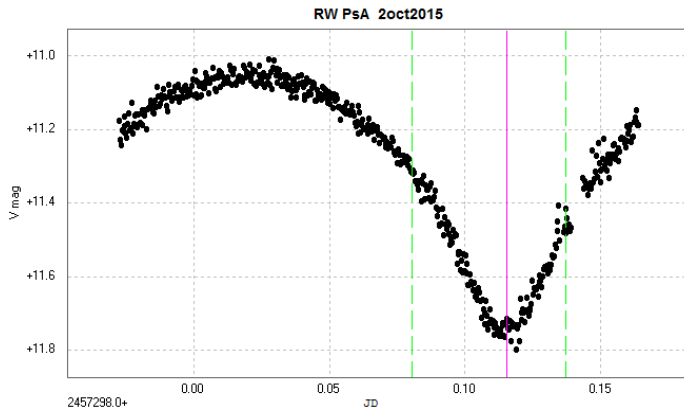


Fig 16 Frequency plot of BC Gru showing dominant frequency

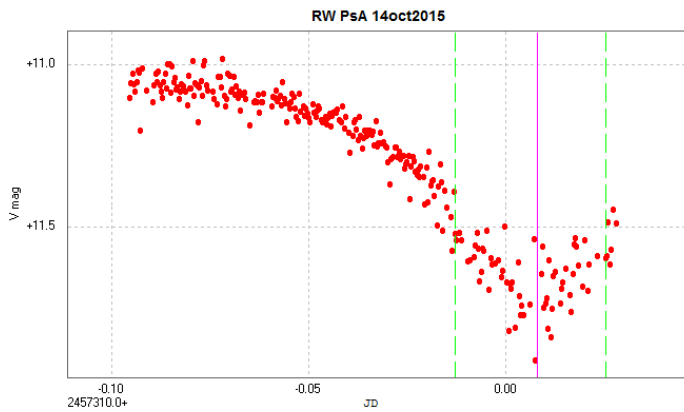
• **RW PsA**



RW PsA

ToM (pri) HJD	Ephemeris HJD ₀	O-C (d)	Vmin (pri)	Vmax
2457298.11804	2457298.16161	-0.04357	11.74	11.05
+/-0.00005			+/-0.004	+/-0.004

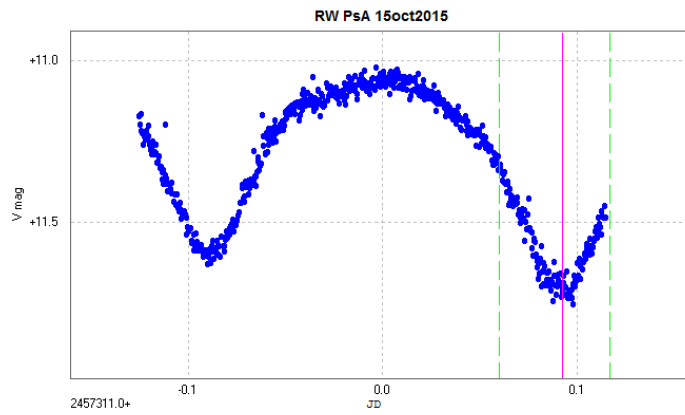
Fig. 17 Lightcurve plot and measures of RW PsA 2 Oct 2015



RW PsA

ToM (pri) HJD	Ephemeris HJD ₀	O-C (d)	Vmin (pri)	Vmax
2457310.01056	2457310.05647	-0.04591	11.75	11.07
0.00011			+/-0.02	+/-0.02

Fig. 17 Lightcurve plot and measures of RW PsA 14 Oct 2015



RW PsA

ToM (pri) HJD	Ephemeris HJD ₀	O-C (d)	Vmin (pri)	Vmax
2457311.09451	2457311.13782	-0.04331	11.69	11.05
0.00008			+/-0.01	+/-0.01

Fig. 18 Lightcurve plot and measures of RW PsA 15 Oct 2015

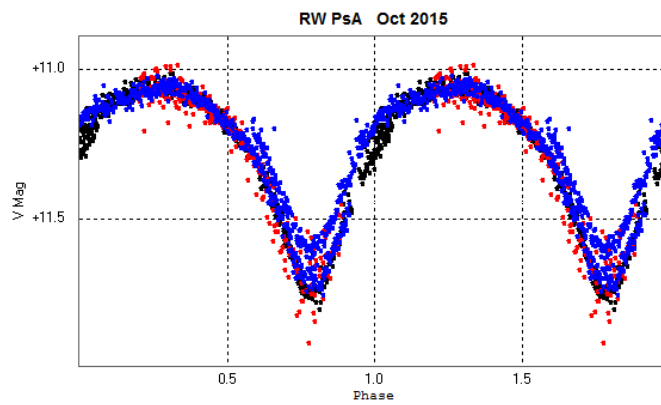


Fig.19 Phase plot of RW PsA

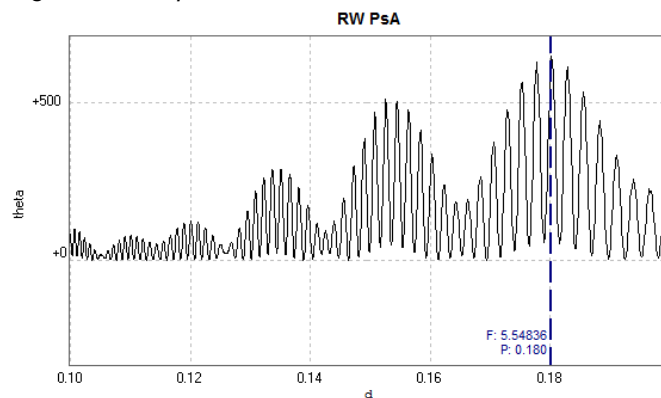


Fig. 20 Frequency plot of RW PsA showing dominant frequency

- Summary of results

V* Star	HJD	Period(d)	Error(+/-)	O-C(d)	Vmax	Vmin (pri)	Vmin (sec)	Error (+/-)
RV Gru	2457274.08904	0.259582	0.00024	0.009	11.07	11.75	11.66	0.02
BC Gru	2457277.15343	0.307297	0.00062	0.059	10.59	10.99	10.94	0.01
RW PsA	2457311.09451	0.360470	0.00099	-0.043	11.06	11.73	11.59	0.01

AAVSO VSX

V* Star	HJD ₀	Period(d)	Vmax	Vmin(pri)
RV Gru	2452500.2789	0.259519	11	11.4
BC Gru	2448479.9266	0.307357	10.6	10.94
RW PsA	2452500.2090	0.360451	11.05	11.76

Table 16 Summary of measured (top half) and published (bottom half) light elements and magnitudes of targets.

Notes:

In Table 16, *HJD* is epoch of best night's ToM for each target as selected on the basis of the smallest error of all measured primary minima. *Period* and *error* shown is derived from dominant frequency and error reported from Peranso's Lomb-Scargle period analysis. *O-C* is the difference between HJD and ephemeris time calculated on the basis of AAVSO VSX published values. It may represent changes in the period since the last.

Epoch (HDJ₀) from AAVSO VSX for RV Gru and RW PsA are 13 Aug 2002, epoch for BC Gru is 11 Aug 1991 (AAVSO-VSXweb)

Extrema V magnitude values shown in Table 16 are the mean of all ToMs and maxima observed for each target.

The large difference between RV Gru measured primary minimum of 11.75V and published Vmin from AAVSO VSX 11.4V appears to be real. The difference between the published and observed values is ten times the measurement uncertainty.

8. Error Analysis

Errors in measurements are divided into two categories: Systematic errors and random errors. In CCD photometry we measure the flux of point sources represented by the counts read from image pixels which are then converted to the apparent magnitude of the target.

Pixel counts contain both the desired signal and unwanted or error signal. The error counts are made up of both random and systematic errors or noise. In stellar

photometry and in general the quality of the image is closely related to the signal to noise ratio (SNR).

For no-filter aperture photometry of stars in the visual band, systematic errors for measurement of apparent magnitude are mainly caused by the accuracy and the number of comparison/reference stars. In this project the accuracy of measurements depended of the availability of sufficient number of measurable (bright enough) photometric reference stars in the image frame. The image frames containing all three target stars had at least 50 UCAC 4 catalogue reference stars, more than sufficient for systematic errors from this source not to be an issue.

Random errors are of easily controlled if the SNR is sufficiently high. The SNR in each pixel is given by the *CCD equation* (Howell 2000) :

$$SNR = N_*/(N_* + n_{pix}(N_s + N_d + N_r^2))^{1/2}$$

Where N_* is the total count from the target object, the wanted signal

n_{pix} is number of pixels inside the aperture circle.

N_s is sky background count/pixel

N_d is dark current (thermal noise)/pixel

N_r is total read noise /pixel

In practice, because the target stars were relatively bright, the only significant contribution to the noise in the above expression was sky noise caused by sky background light, atmospheric turbulence, light clouds and haze. The resulting measurement scatter was controlled by sampling the light curve with sufficient frequency. An imaging rate of one or two images per minute was found to be satisfactory. The uncertainty at any point on the curve was estimated by binning 20 consecutive points and calculating the mean $\langle x_{20} \rangle$ and standard deviation σ_{20} . 20 observations represented only 10 minutes of the lightcurve, short enough that real changes in brightness not to be significant. $\sigma_{20}^{1/20}$ was then used as the uncertainty in the magnitude at that point. The uncertainty at the extrema (minimum or maximum) points was estimated in the same way. Depending on the sky conditions during the observing session, σ_{20} ranged from 0.015 to 0.05. The uncertainty therefore ranged from 0.003 to 0.02 magnitudes approximately.

9. Conclusions

The objectives of this project were achieved. The preferred experimental method included three evenly spaced (one every 2-3 weeks) observing sessions over the available observability season (Richards 2015b). For the targets selected this didn't quite coincide with the semester time frame. Of the three targets only RV Gru met this criterion. The other two targets observed at uneven intervals and RW PsA only over two weeks. Despite the short intervals and limited phase coverage all results were pleasingly consistent with published values with period differences ranging from 2 to 6 seconds in the 6 to 8 hour published periods. These differences are well within the

uncertainties given by the Peranso software. Extrema magnitude results are also consistent with published values and within the uncertainties listed in the tables i.e. all magnitudes of maxima and minima are within 0.03 magnitude of published figures. The one exception is RV Gru primary minimum. There is a 0.35V difference between the mean of three observations spanning 32 days, that are internally consistent within +/- 0.02V, and that of the published value. This difference appears to be real and warrants further investigation.

References:

- AAVSOweb: <https://www.aavso.org/>
 AAVSO-VSXweb: <https://www.aavso.org/vsx/>
 AstrometricaWeb: <http://www.astrometrica.at/>
 Binnendijk, L. 1965, *VeBam* 27, 36B
 BritastroWeb: http://britastro.org/computing/applets_dt.html
 Csizmadia, Sz. & Klagyivik, P. 2004, *A & A* 426, p1001-1005
 Howell, S. 2000, *Handbook of CCD Astronomy*.
 Kreiner, J. et al. 2000 *Atlas of O-C diagrams of Eclipsing Binary Stars*
 Lucy, L. 1968, *ApJ*, 153,8,77L
 Lucy, L & Wilson, R. 1979, *ApJ*, 231,502
 Mikulasek, Z. et al. 2013 preprint [arXiv:1311.0207](https://arxiv.org/abs/1311.0207)
 MtSohuraWeb: <http://www.as.up.krakow.pl/o-c/>
 Ostlie, D. and Carroll, B. 2007, *An Introduction to Modern Stellar Astrophysics* 2nd ed.
 Pribulla, T. et al. 2003, *CoSka*, 33, 38P
 Raab, H 2015 Personal communication
 Richards, T. 2015a, *VSS Newsletter* 2015-3, 12P
 Richards, T. 2015b, Personal communication
 Vanmunster, T. 2004 *Peranso Users Manual*
 VSS-EW-web: <http://www.variablestarsouth.org/research/variable-types/eclipsing-binaries?id=1007>
 Wilson, R. 2001, *IBVS* 5076, IAU commission 27 & 42
 Wilson, R. & Devinney, E. 1971, *AJ* 166, 605

Catalogues and databases

- GCVS (General Catalogue of Variable Stars) <http://www.sai.msu.su/gcvs/gcvs/iii/html/>
 AAVSO Variable Star Index (VSX) <https://www.aavso.org/vsx/>
 Czech Astronomical Society http://var2.astro.cz/EN/brno/eclipsing_binaries.php
 Kreiner, J. et al. 2000 *Atlas of O-C diagrams of Eclipsing Binary Stars* <http://www.as.up.krakow.pl/o-c/>

Observing Logs***Eclipsing Binaries Project Log***

Date observed	UT start	Images taken	Exposure (sec)	Interval (sec)	Ambient temp	Sky condition	Comment
<i>RV Gru</i>							
8/09/2015	1151	360	8	30	15	Clear	very good nighth
	1453	360	8	30	14	Clear	
	1758	40	8	30	12	Clear	
27/09/2015	0909	360	8	60	15	Clear/humid	
9/10/2015	0855	130	8	30	17	cloudy	aborted after 1hr
10/10/2015	1215	360	8	30	17	Clear	Clear
	1518	120	8	30	17	Clear	Clear
<i>BC Gru</i>							
9/09/2015	0920	60	5	15	15	clear	aborted at 1440
	0954	360	6	15		clear	
	1129	360	6	30		clear	
	1429	30	6	30		cloudy	
10/09/2015	0905	180	6	30	16	clear->cloudy	aborted after 1.5hrs
11/09/2015	0844	20	7	30	17	clear	Clear all night
	0903	360	7	30		clear	
	1204	500	7	30		clear	
	1614	100	7	30		clear	
28/09/2015	0846	10	8	15	16	clear	
	0856	50	7	30			
	0923	416	6	30		clear->cloudy	aborted by clouds
	1311	360	6	30		clear	
16/10/2015	0905	20	5	15	19	clear	too much scatter
	0933	20	6	15		clear	too much scatter
	0956	20	6	60		clear	
	1027	20	15	60		clear	changed to 2x2 binning
	1045	20	15	60		clear	2x2 binning
	1109	270	15	60		clear	
<i>RW PsA</i>							
2/10/2015	1120	480	8	30	19	clear	clear all night
	1525	60	8	30			
14/10/2015	0942	480	8	30	15	clear-	

						>cloudy	
15/10/2015	0858	630	8	30	17	clear	
	1515	60	8	30			